

Nanotube-derived carbon foam for hydrogen sorption

Feng Ding, Yu Lin, Pavel O. Krasnov, and Boris I. Yakobson^{a)}

Department of Mechanical Engineering and Materials Science, Department of Chemistry, and The Richard E. Smalley Institute for Nanoscale Science and Technology, Rice University, Houston, Texas 77005, USA

(Received 15 June 2007; accepted 4 September 2007; published online 22 October 2007)

A new kind of carbon foam, which is based on the welding of single-walled carbon nanotubes, is built in a computer simulation. Its precisely defined architecture and all atomic positions allow one to perform detailed theoretical analysis of the properties. Such foam is as light as 1/9 of steel, while its stiffness is similar and nearly isotropic, and it represents a strong three-dimensional material with various possible applications. Furthermore, its nanoporous structure is accessible to molecular hydrogen and the potential surface analysis indicates that it should be an excellent hydrogen storage medium. Importantly, such foam is a feasible structure that can be produced based on the known tube/fullerene welding techniques. © 2007 American Institute of Physics.

[DOI: [10.1063/1.2790434](https://doi.org/10.1063/1.2790434)]

I. INTRODUCTION

Utilizing hydrogen for portable energy storage at feasible conditions (not too remote from the ambient) requires material carriers which presently do not exist. Confining H fuel without the exceeding weight of the material carrier and yet in a relatively small volume presents both a fundamental challenge and a task of great practical importance. The application goals for hydrogen storage are set at $g > 6$ wt % for gravimetric and $v > 45$ kg/m³ for volumetric measures, to be reached by 2010. On the other hand, Dewar's liquid hydrogen density of about $v = 70$ kg/m³ can hardly be surpassed in any adsorbed form. Therefore a relatively light storage medium/support with the density $\rho_s = v/g < \sim 1$ g/cm³ is required for achieving such goals in order for volumetric capacity to match reasonable gravimetric capacity.

Empirical trial-and-error search can lead to breakthroughs but can also be prohibitively expensive. Developing comprehensive theoretical approach or a combination of modeling tools should help evaluate and design the desired materials. Among the desired properties, several major features stand out and define the challenge. One can distinguish (i) the binding energy requirement on one hand, and (ii) weight and (iii) volume requirements, on the other. Additionally, issues of the (iv) kinetics, i.e., sufficiently fast diffusion pathways for the fueling and release, and (v) thermal management, removal of excessive heat at the exothermic fueling stage, should also be kept in mind.

Carbon nanotube (CNT) materials are expected to be one of the few best candidates for hydrogen storage due to the high surface-to-volume ratio and light porous structure.¹ However, raw CNT materials often form bundles and the hydrogen storage in such tube bundle was found to be very low.² Theoretical analyses indicate that the short tube-tube separating distance [van der Waals (vdW) gap] in the tube

bundle (0.34 nm) prevents hydrogen molecule from accessing the space between the tubes.³ Based on this analysis, a theoretical suggestion of increasing the vdW gap to ~ 0.7 nm was proposed as a way to enhance the CNT storage.^{2,3}

Interesting and active studies on carbon nanohorns also demonstrate that the presence of highly curved corners and pores can significantly improve the physical sorption, when the synergetic contribution and superposition of H₂-H₂ and H₂-C vdW forces can play a positive role. Among several reports, at least two recent papers emphasize this special advantage,⁴ although the exact location and the nature of the stronger bonding need further exploration.

A new theoretical consideration suggests that placing of parallel graphene layers every 0.7 nm could double the potential well depth for hydrogen adsorption and significantly enhance the hydrogen storage capacity at room temperature.⁵ Unfortunately, such an ideal structure would certainly be unstable in reality, and can only serve as a guiding model.

Beyond pure carbon substrates, recent theoretical studies show that, with suitable metal doping to CNT or fullerene surface, the DOE goal can be possibly achieved at room temperature,⁶ whereas how to prevent the doped CNTs or fullerenes from aggregation remains unknown and may become a significant predicament.

Among the above possible ways to enhance hydrogen storage, designing a stable, light carbon-nanotube-based material with numerous ~ 1 nm pores seems the key to further improvements and practical application. Earlier, various carbon foam structures were produced experimentally⁷ and proposed theoretically.^{8,9} Experimentally produced foams often have very large pores inside (e.g., 10–100 nm) which do not match the hydrogen storage needs. On the other hand, although some of the computer-designed foams appear very stable and perhaps perfect for hydrogen storage due to the large population of ~ 1 nm pores, even conceptually/theoretically, there is no clear way to produce them (from experimentally available components). For example, “buck-

^{a)}Author to whom correspondence should be addressed. Electronic mail: biy@rice.edu

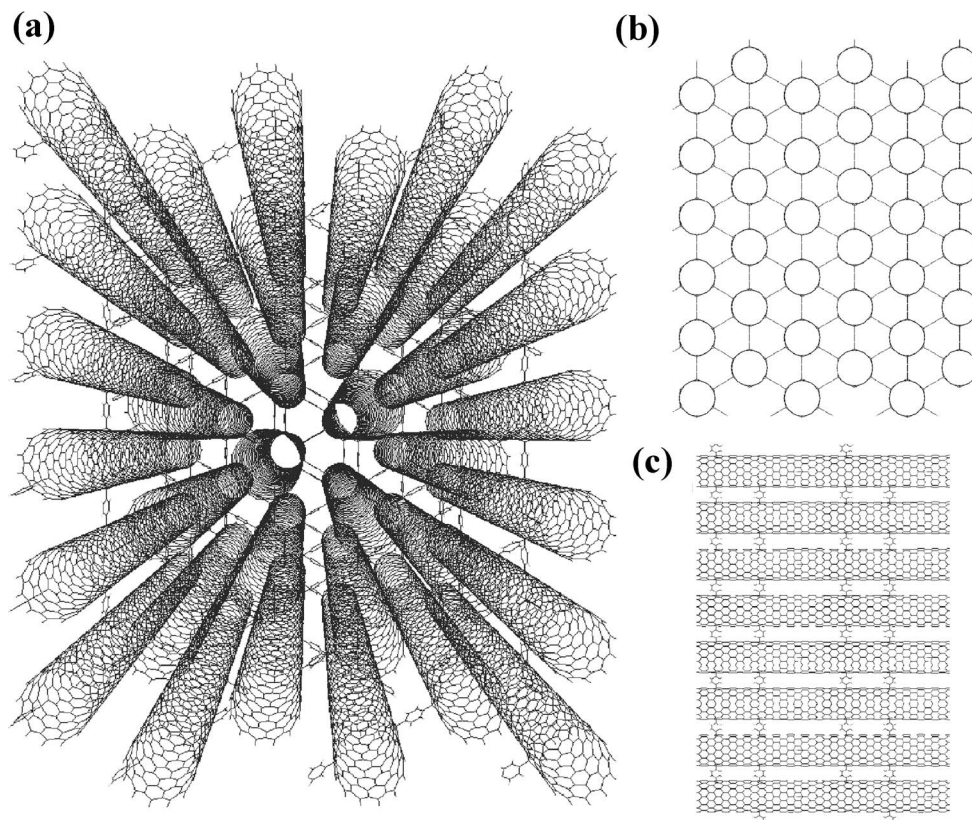


FIG. 1. SWCNT bundles functionalized with *p*-phenylene. The neighboring tubes in the bundle are separated by benzene functional group and the vdW gap is kept at 0.67 nm. (b) and (c) show top and side views of the well-separated bundle.

ygym” structure⁹ was made from fullerene lattice of diamond symmetry, which is far from the natural close-packed fullerene bulk materials.

In contrast, in this paper a new carbon foam structure was designed theoretically based on the known welding technique applied to the crossing CNT arrays. The resulting foam structure is less anisotropic than a parallel array, stable, and almost stiff as steel in all directions. Furthermore, the widely present pores in this foam structure promise an excellent hydrogen storage ability of such medium. Theoretical analyses indicate that its hydrogen storage capacity is beyond the limit of the optimally separated tube bundles. Mainly for this comparison, we begin discussion below from this kind of well-separated nanotube array, where the separation between the tubes is maintained by the present chemical spacers—functional chemical groups attached to and cross-linking the neighboring tubes. Then the physical way of cross-linking nanotube arrays by their welding is discussed in detail, where we show a feasible path (following our earlier work) of fusing the crossing tubes and thus opening the channel between their interiors. After that, we briefly analyze the basic properties of the resulting three-dimensional foam, its electronic structure, mechanical stability, and the elastic moduli. Next, the ability for retaining H₂ is estimated by computing the potential energy landscape for a H₂ molecule placed inside such foam and evaluating the relative amount of energetically favorable space.

II. COVALENT CROSS-LINKED NANOTUBE ARRAY

A possible experimental route to achieve the well-separated single-walled carbon nanotube (SWCNT) bundles is via chemical functionalization, which is covalent attachment of the functional groups to the adjacent tubes in the array bundle. With certain concentration, such functional

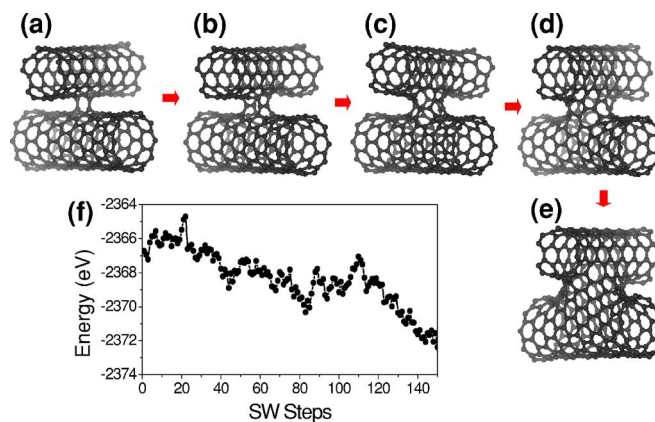


FIG. 2. (Color online) Welding of two crossing tubes. Simulation starts with a (5,5) tube and a (10,0) tube that are connected by two C–C bonds (a). Then an energetically preferred C–C bond was rotated (SW transformation) and the whole structure was relaxed at each step. Here (b)–(d) are the snapshots between the initial structure and the final structure, and (e) is the complete junction after 150 step bond rotation. Panel (f) shows the changes of structural energy during the welding process. The simulation was performed with the Tersoff-Brenner potential (Ref. 14).

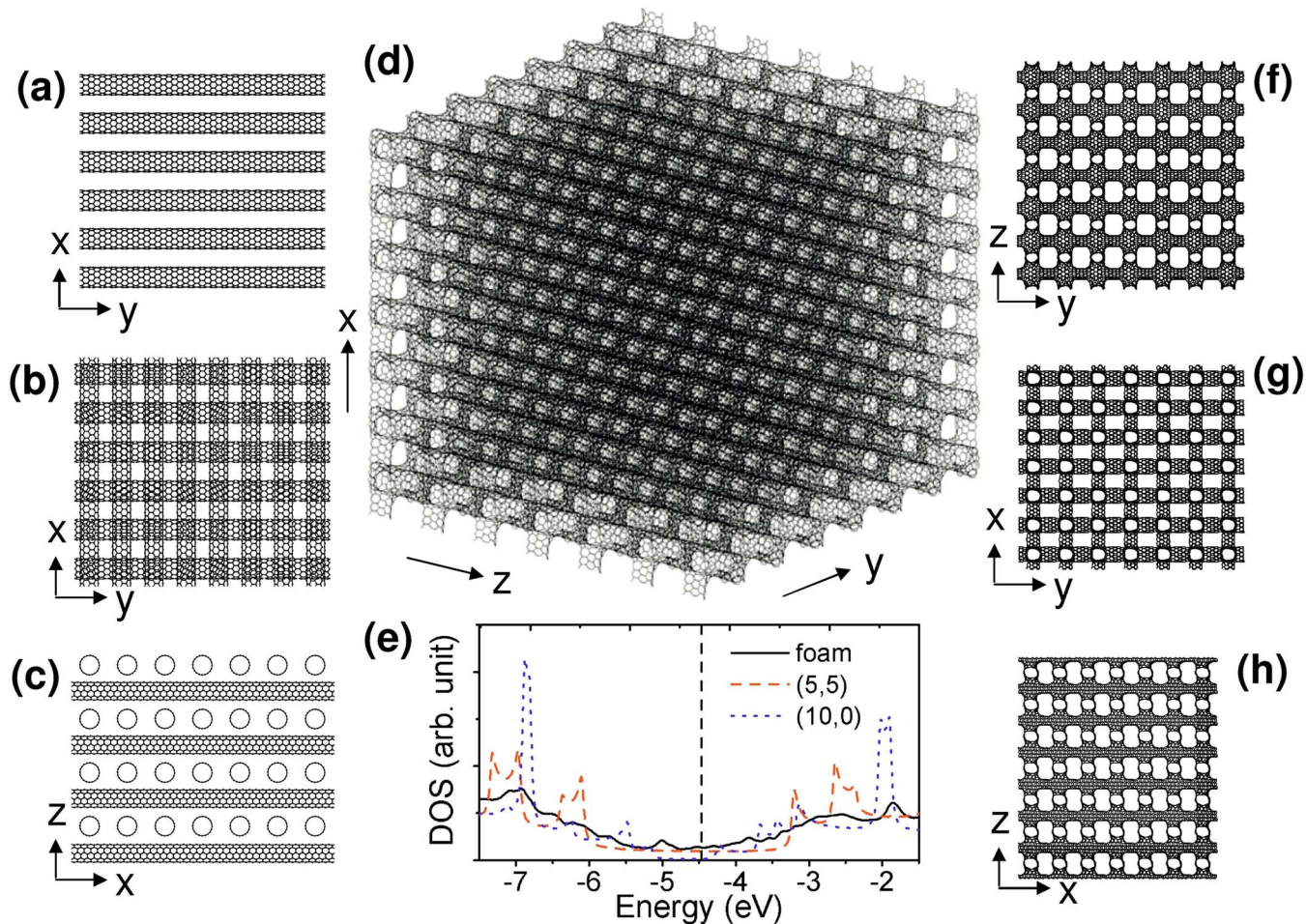


FIG. 3. (Color online) CNT-based carbon foam structure. (a)–(c) show the steps of stacking a three-dimensional SWCNT matrix. Then the welding of each cross-contact in the matrix will produce a foam as shown in (d). (e) is the electronic density of states (DOS) of the foam compared to the set of (5,5) and (10,0) SWCNTs. (f)–(h) show the three orthogonal aspect views of the foam structure.

groups should be able to overcome the vdW attraction between tubes (typically ~ 1 eV/nm of length) and thus increase the tube-tube distance.¹⁰ Figure 1 shows such first proposed^{11,12} and actually computed (full relaxation, with density functional based tight-binding method) model of a biphenyl¹¹ and *p*-phenylene functionalized SWCNT bundle. In the well-separated array, the vdW gap was maintained at the nearly desirable value of 0.67 nm (wall to wall) by adding *p*-phenylene functional groups. This makes two improvements relative to usual CNT bundles: it makes the surface of the tubes accessible, and in addition the overlap of vdW potential should nearly double the binding energy in these locations. However, the interior of the tubes still remains in disadvantage, essentially disconnected from the ambient gas and therefore lost for the storage function. In the attempt to connect the exterior and interior surfaces of an individual tube, we recall the process of welding. The next section describes its essence and how it allows building of a fully accessible three-dimensional (3D)-foam structure.

III. CARBON FOAM STRUCTURE THROUGH NANOTUBE WELDING

The element of the 3D foam is a single crossover of two nanotubes. Figure 2 shows a simulation process of welding a

tube-tube cross junction. Initially, two C–C bonds were created between two cross SWCNTs [see Fig. 2(a)]. By 90 rotations of the most energetically preferred bonds [Stone-Wales (SW) transformation] located around the junction, the neck between the two tubes grows thicker and thicker and a complete welded junction is eventually formed, after 150 SW steps in Figs. 2(a)–2(e). The total energy decreases by about 5–6 eV after such a junction forms [Fig. 2(f)]. In agreement with Euler's rule,¹³ the complete junction contains 12 heptagons (see the Appendix).

Now, the SWCNTs can be stacked up into a 3D matrix as shown in Figs. 3(a)–3(c). Exposure to heat and/or radiation leads to the welding and creates the junctions of the type shown in Fig. 2(e) at each cross point in the matrix. Eventually, a beautiful carbon foam structure is created [Fig. 3(d)]. From Figs. 3(f)–3(h), the three aspect views of the foam, one can see that there is a large number of ~ 1 nm pores in such foam, and they are all interconnected by the channels and therefore fully accessible for sorption.

It is important to note that although the foam shown in Fig. 3(d) is a theoretical model of previously proposed foam structures,^{8,9} in this case the path/mechanism to its formation is shown, not just the final organization as in Refs. 8 and 9. There are two key steps to achieve such a structure: the ar-

chitecture of the stacked tubes and the tube welding technique. Although the exact structure like Fig. 3(c) is not achieved yet, the experimental methods of carbon nanotube alignment are well established¹⁵ and separating the tubes from each other by a certain distance and stabilizing them are expected to be achieved by chemical functionalizations.¹⁰ The welding technique of CNTs and related structures is known as a practical process today. For example, coalescence of encapsulated fullerenes in SWCNT (carbon peapods) into double-walled CNTs by thermal annealing was studied extensively for quite a few years^{16,17} and the X shape junctions as in Fig. 2(e) have been studied well both theoretically and experimentally.^{18,19} So, if one has a carbon matrix like in Fig. 3(c) or even a somewhat randomized SWCNT matrix, a suitable thermal treatment or electron/ion irradiation at elevated temperature will create the foam structures topologically similar to that in Fig. 2(d). Thus, such foam structure is likely to be produced in the near future as the CNT technology rapidly progresses. Recent experimental report of the zeolitelike carbon structure²⁰ serves as an encouraging example. It is important to evaluate the basic properties of the generic nanotube-derived foam: electrical, mechanical, and its ability to retain molecular hydrogen.

IV. PROPERTIES

A. Electronic structure

While the welding algorithm does establish the connectivity of the atoms and the covalent bond lattice, the exact geometry of the nanotube-based foam should be obtained by relaxation. Here it was performed using the TROCADERO package²¹ via density functional based tight-binding method.²² Since the computational cell contains 320 carbon atoms, only Γ point energy is computed during the relaxation, while a $7 \times 7 \times 7$ Monkhorst-Pack k -point mesh is employed for the electronic density of states (DOS) calculation.

In Fig. 3(e), the solid line shows the normalized DOS of the foam. For comparison, similarly normalized DOSs of pristine (5,5) and (10,0) SWCNTs are calculated and also shown in Fig. 3(e) in dashed line and dotted line, respectively. Surprisingly, the DOS of carbon foam has a finite value at the Fermi level, and the density is even higher than the density of the pristine armchair (5,5) tube at the Fermi level. These results should be confirmed by further relaxation with denser k -point mesh or even higher level calculations such as *ab initio* methods, which is beyond the scope of this report. In the foam structure, a substantial part of the π system of (5,5) tubes remains intact, and the Fermi level difference between (5,5) and (10,0) tubes causes the electronic band overlap and the electron redistribution. Consequently, the DOS gap of (10,0) disappears when (10,0) tubes are welded with (5,5) tubes. Although the DOS at the Fermi level of the foam structure might be depressed by using denser- k -point mesh or a more accurate method, we do not expect that the gap will open up. Additionally, one-dimensional (1D)-type van Hove singularities all disappear when the foam structure is formed, which also indicates that the degeneracy of electronic levels is destroyed, and electrons redistribute within the foam.

B. Mechanical properties

CNT is expected to have many important future applications due to its distinguished mechanical, electrical, and chemical properties.²³ For example, CNT's failure strength along the tube axis direction may be up to hundred times of steel's,²⁴ which promises CNT as the strongest light (the CNT's density is just 1/6–1/3 of iron's) materials in nature. Materials as strong as CNT are useful for a variety of applications, such as new generation of machines, vehicles, aircrafts, and space structures,¹³ whereas, 1D structure limits the application as strong bulk material because of the weak tube-tube interaction. For example, Young's modulus of carbon nanotube bundle along the direction perpendicular to the tube axis is just in the order of 10 GPa, which is $\sim 1/100$ of that along the tube axial direction, ~ 1 TPa. To overcome this problem, CNTs are added to polymer or other composites in order to produce compounds with enhanced mechanical properties.²⁵ Although the mechanical properties of the CNT-added compounds may be significantly improved, they are far from the limit of CNT. In order to achieve bulk materials as strong as CNT, new techniques of treating CNT are needed.

Different from tube bundles and the SWCNT matrix as shown in Fig. 3(c), the foams are connected by strong covalent C–C bonds in all three directions. The calculated Young's moduli (110, 180, 130 GPa along the x, y, z directions as shown in Fig. 2) and Poisson ratios (0.16, 0.18, 0.10 along the x, y, z directions) show that it is a rather isotropic structure compared to SWCNT bundles and graphite. Although, due to the porous structure, the foam's Young's modulus is about one order lower than that of SWCNT, it still should be a rather strong material. More importantly, the foam has very similar mechanical properties along all directions. Even along the direction perpendicular to the aligned SWCNTs (z direction as shown in Fig. 3), high density covalent C–C bonds in the tube-tube necks ensure high strength as that along the other two directions. That is proved by the fact that the Young's modulus along this direction was increased by one order. Together with its very light structure [the density of the foam shown in Fig. 3(d) is 0.93 g/cm³, only 1/9 of iron or 1/3 of aluminum], it may have broad industrial and scientific applications in the future.

C. Hydrogen adsorption potential analysis

Except for its interesting electrical and mechanical properties, the porous structure makes the nanofoam an exceptional hydrogen storage medium. As seen in Figs. 3(e)–3(g), the foam has numerous pores of 0.7–1.0 nm. Different from carbon nanotube bundles, the whole (both sides) graphene surface in the foam is accessible for hydrogen molecules, and thus its geometrical surface area is close to that of the ideal graphene layer.

Figure 4 shows the distribution of H₂ host energy in the foam compared to that in carbon nanotube bundles with various vdW gaps. Lennard-Jones potential in "12-6" form [parameters: $\epsilon=3.69$ meV and $\sigma=0.297$ nm (Ref. 26)] is used to describe the H₂–C interaction. For the normal bundle with 0.34 nm vdW gap, the spaces between neighboring tubes are

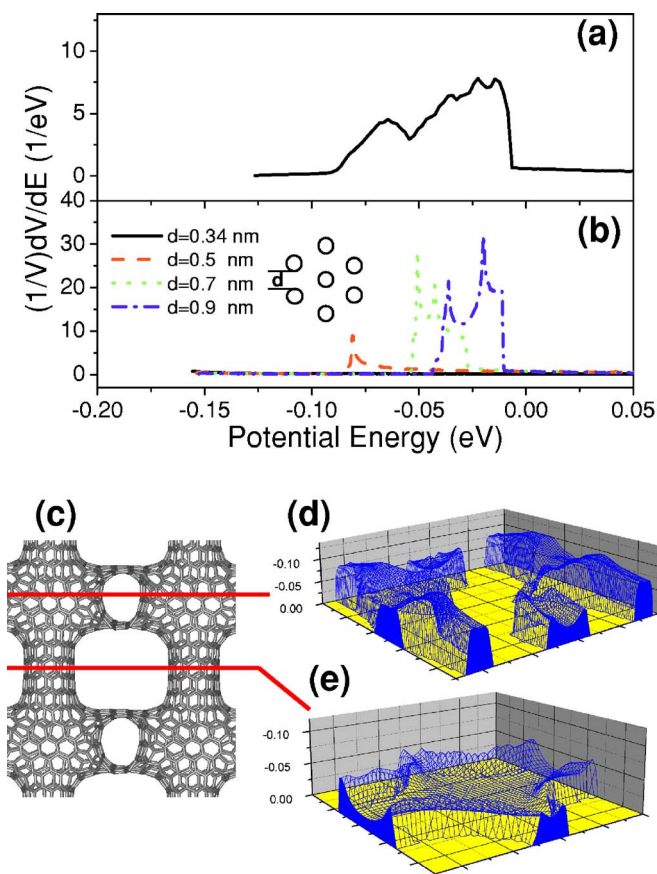


FIG. 4. (Color online) Spectrum of potential energy of molecular hydrogen adsorption in the (a) foam compared to those in (b) (5,5) tube bundles with various van der Waals gaps (b). Panels (d) and (e) show two potential maps in two cross sections of the foam (c). Only part of the spectrum which corresponds to negative adsorption is shown for clarity.

too tight to host any hydrogen. For the bundles with vdW gaps of 0.5 and 0.9 nm, either has very small effective volume fraction (the fraction of volume with negative adsorption energy, $E < 0$, where H_2 is attracted) or has very low adsorption energy. This is in agreement with atomic simulations,^{2,3} showing that the tube bundle with vdW gap ~ 0.7 nm has the best hydrogen storage capacity because of its relatively high adsorption energy and large effective accessible volume fraction. However, even such best-separated tube bundle does not have any advantage over the foam structure. The foam structure has larger effective adsorption volume fraction ($\sim 40\%$ vs $\sim 30\%$ in the best bundle) and higher adsorption energy (more than 12% volume with adsorption energy < -0.05 eV vs $\sim 10\%$ volume with adsorption energy around -0.05 eV) than the bundle with 0.7 nm vdW gap. The host energy maps in the foam [Figs. 4(c)–4(e)] indicate that the space around the tube-tube junction corresponds to the high adsorption energy peak in Fig. 3(a), which hints that the foam structure can be further optimized for even better hydrogen storage. One can say that the foam is the best considered stable pure carbon structure for hydrogen storage, whose storage capacity should be close to the recently studied optimally separated graphene layers.⁵

Besides the pure physical adsorption, the chemical adsorption of hydrogen in carbon nanotube is an important alternative or supplementary way for achieving the DOE

goals.^{27,28} Normally, transition metal catalysts are required to decompose the molecular hydrogen.²⁷ Here we also note that the foam is an exceptional medium for chemical adsorption and for metal doping. In addition to its fully accessible surface, the topologically imposed 12 heptagons around each tube-tube junction make the foam chemically more active for hydrogen atoms or/and for holding metal atoms while preventing their aggregation.

V. CONCLUSION

A new carbon foam structure is designed based on the tube-tube welding technique. For one precisely defined example, the calculations and analysis show that such foam is strong and light, which promises a number of important applications as bulk material. Besides the distinguished mechanical properties, the adsorption energy distribution in the foam structure indicates excellent potential hydrogen storage capacity, which should be further verified by direct simulations (e.g., grand-canonical Monte Carlo). More importantly, based on the rapid progress of carbon nanotube technology, such foam structure can be produced in the near future through radiation welding, template synthesis,²⁰ or in some other ways. The question “Can we make new carbon-based 3D networks that outdo zeolites?” posed by Smalley nearly two decades ago²⁹ may just be getting a positive answer.

ACKNOWLEDGMENTS

This work was supported by the DOE Hydrogen Sorption Center of Excellence, Contract No. DE-FC36-05GO15080, and partially by the Office of Naval Research (program manager Peter Schmidt). We are grateful to Yury Gogotsi for timely pointing to a useful publication.²⁰

APPENDIX: EULER’S RULE IN sp^2 CARBON NETWORK AND TUBE-TUBE JUNCTION

We want to comment on why the minimum number of heptagons at the tube crossing is 12. This can be viewed as a corollary of a more general yet elegant analysis in Ref. 30. However, for one particular case of tube crossing, this follows easily after we derive a useful simple relationship, which in turn follows from Euler’s rule applied specifically to the sp^2 carbon networks, such as fullerenes, nanotubes, or other shell-type architectures. For these systems, two properties should be additionally utilized: (i) each atom has exactly three bonds, and (ii) hexagons are the most common and abundant, while other polygonal faces appear relatively rarely, as “defects.” For a structure without any holes (i.e., genus zero³⁰), according to Euler’s rule, for any polyhedron,

$$V - E + F = 2, \quad (\text{A1})$$

where V , E , and F are the numbers of vertices (atoms), edges (bonds), and faces, respectively, on a polyhedron.

Here we are interested not in the total number F of polygonal faces but rather in the particular quantities n_p of specific p -ring polygons. Obviously,

$$F = \sum n_p. \quad (\text{A2})$$

Further, each p -ring face is enclosed by p edges, while each edge is shared by two faces. Therefore,

$$2E = \sum pn_p. \quad (\text{A3})$$

Finally, and the only specific for sp^2 carbon condition, each vertex (atom) is shared by three adjacent faces, so that

$$3V = \sum pn_p. \quad (\text{A4})$$

(One can note that $2E=3V$.) Substitution of Eqs. (A2)–(A4) into Eq. (A1) yields a simple formula for the numbers of p polygons in the sp^2 network:

$$\sum (6-p)n_p = 12 \text{ or } \sum' (6-p)n_p = 12, \quad (\text{A5})$$

where in the latter version Σ' explicitly omits hexagonal faces ($p \neq 6$).

For a normal fullerene which contains only pentagons and hexagons ($p=5,6$), Eq. (A5) immediately yields $n_5=12$, a well known property that “good” fullerene contains exactly 12 pentagons independent of its size and shape. SWCNT with both ends closed can be viewed as an elongated fullerene, and the number of pentagons on each closing cap is half of that in a fullerene, that is, 6. As a simple illustration, one can easily verify Eq. (A5) for the sp^2 platonic solids: tetrahedron with $p=3$, $n_3=4$; cube with $p=4$, $n_4=6$; dodecahedron $p=5$, $n_5=12$.

For the T-or Y-type SWCNT junctions, each of the three diverging SWCNT branches is terminated by a cap with six pentagons, that is, total $n_5=18$. When only heptagons or octagons are present at the junction as nonhexagonal defects, we have $n_7+2n_8=6$, and possible numbers of heptagons and octagons include $(n_7, n_8)=(6, 0), (4, 1), (2, 2), (0, 3)$. With the “least strained” polygon case, there should be at least six heptagonal imperfections, $n_7=6$.

Similarly, for X shape SWCNT junctions in the welded foam, $n_7+2n_8=12$ since 24 pentagons are necessary to terminate all four of SWCNT branches. Thus the number of heptagons around the junction must be 12 if no other non-hexagonal rings are present.

¹A. C. Dillon, K. M. Jones, T. A. Bekkedahl, C. H. Kiang, D. S. Bethune, and M. Heben, *Nature (London)* **386**, 377 (1997).

²J. Miyamoto, Y. Hattori, D. Noguchi, H. Tanaka, T. Ohba, S. Utsumi, H. Kanoh, Y. A. Kim, H. Muramatsu, T. Hayashi, M. Endo, and K. Kaneko, *J. Am. Chem. Soc.* **128**, 12636 (2006).

³V. V. Simonyan, P. Diep, and J. K. Johnson, *J. Chem. Phys.* **111**, 9778 (1999); Q. Wang and J. K. Johnson, *J. Phys. Chem. B* **103**, 4809 (1999).

⁴H. Tanaka, H. Kanoh, M. Yudasaka, S. Iijima, and K. Kaneko, *J. Am. Chem. Soc.* **127**, 7511 (2005); F. Fernandez-Alonso, F. J. Bermejo, C. Cabrillo, R. O. Loutfy, V. Leon, and M. L. Saboungi, *Phys. Rev. Lett.* **98**, 215503 (2007).

⁵S. Patchkovskii, J. S. Tse, S. N. Yurchenko, L. Zhechkov, T. Heine, and G. Seifert, *Proc. Natl. Acad. Sci. U.S.A.* **102**, 10439 (2005).

⁶Y. Zhao, Y.-H. Kim, A. C. Dillon, M. J. Heben, and S. B. Zhang, *Phys. Rev. Lett.* **94**, 155504 (2005); T. Yildirim and S. Ciraci, *ibid.* **94**, 175501 (2005).

⁷A. V. Rode, E. G. Gamaly, A. G. Christy, J. G. F. Gerald, S. T. Hyde, R. G. Elliman, B. Luther-Davies, A. I. Veinger, J. Androulakis, and J. Giapintzakis, *Phys. Rev. B* **70**, 054407 (2004); A. Cao, P. L. Dickrell, G. Sawyer, M. N. Ghasemi-Nejhad, and P. M. Ajayan, *Science* **310**, 1307 (2005).

⁸A. L. Mackay and H. Terrones, *Nature (London)* **352**, 762 (1991); K. Umemoto, S. Saito, S. Berber, and D. Tomanek, *Phys. Rev. B* **64**, 193409 (2001).

⁹D. Vanderbilt and J. Tersoff, *Phys. Rev. Lett.* **68**, 511 (1992).

¹⁰B. K. Price and J. M. Tour, *J. Am. Chem. Soc.* **128**, 12899 (2006).

¹¹Y. Lin *et al.* (unpublished); B. I. Yakobson and R. Hauge, in: “The DOE Hydrogen Program 2006 Annual Progress Report, May 2006, Arlington, VA,” p. 483 see: http://www.hydrogen.energy.gov/pdfs/progress06/iv_c_lj_yakobson.pdf.

¹²P. F. Weck, E. Kim, N. Balakrishnan, H. Cheng, and B. I. Yakobson, *Chem. Phys. Lett.* **439**, 354 (2007).

¹³B. I. Yakobson and R. E. Smalley, *Am. Sci.* **85**(4), 324 (1997).

¹⁴D. W. Brenner, *Phys. Rev. B* **42**, 9458 (1990).

¹⁵S. Huang, B. Maynor, X. Cai, and J. Liu, *Adv. Mater. (Weinheim, Ger.)* **15**, 1651 (2003); S. G. Rao, L. Huang, W. Setyawan, and S. Hong, *Nature (London)* **425**, 36 (2003).

¹⁶Y. Zhao, R. E. Smalley, and B. I. Yakobson, *Phys. Rev. B* **66**, 195409 (2002).

¹⁷B. W. Smith and D. E. Luzzi, *Chem. Phys. Lett.* **321**, 169 (2000).

¹⁸F. Cleri, P. Keblinski, I. Jang, and S. B. Sinnott, *Phys. Rev. B* **69**, 121412 (2004).

¹⁹M. Terrones, F. Banhart, N. Grobert, J.-C. Charlier, H. Terrones, and P. M. Ajayan, *Phys. Rev. Lett.* **89**, 075505 (2002).

²⁰Z. Yang, Y. Xia, and R. Mokaya, *J. Am. Chem. Soc.* **129**, 1673 (2007).

²¹R. Ruralia and E. Hernández, *Comput. Mater. Sci.* **28**, 85 (2003).

²²D. Porezag, T. Frauenheim, T. Koller, G. Seifert, and R. Kashner, *Phys. Rev. B* **51**, 12947 (1995).

²³R. Saito, G. Dresselhaus, and M. S. Dresselhaus, *Physical Properties of Carbon Nanotubes* (Imperial College, London, 1998).

²⁴M. Yu, O. Lourie, M. Dyer, K. Moloni, T. Kelly, and R. S. Ruoff, *Science* **287**, 637 (2000); T. Dumitrica, M. Hua, and B. I. Yakobson, *Proc. Natl. Acad. Sci. U.S.A.* **103**, 6105 (2006).

²⁵X. Wang, N. P. Padture, and H. Tanaka, *Nat. Mater.* **3**, 539 (2004); G.-D. Zhan, J. D. Kuntz, J. Wan, and A. K. Mukherjee, *ibid.* **2**, 38 (2003).

²⁶S. C. Wang, L. Senbetu, and C. Woo, *J. Low Temp. Phys.* **41**, 611 (1980).

²⁷P. C. H. Mitchell, A. J. Ramirez-Cuesta, S. F. Parker, J. Tomkinson, and D. Thompsett, *J. Phys. Chem. B* **107**, 6838 (2003); A. J. Lachawiec, Jr., G. S. Qi, and R. T. Yang, *Langmuir* **21**, 11418 (2005).

²⁸A. Nikitin, H. Ogasawara, D. Mann, R. Denecke, Z. Zhang, H. Dai, K. Cho, and A. Nilsson, *Phys. Rev. Lett.* **95**, 225507 (2005).

²⁹R. E. Smalley, *Acc. Chem. Res.* **25**, 98 (1992).

³⁰V. H. Crespi, *Phys. Rev. B* **58**, 12671 (1998).